Rev.Adv.Mater.Sci. 5 (2003) 178-182

MODIFICATION OF METAL NANOPARTICLES IN SiO_2 BY THERMAL OXIDATION

H. Amekura, Y. Takeda, K. Kono, H. Kitazawa and N. Kishimoto

Nanomaterials Laboratory, National Institute for Materials Science, 3-13 Sakura, Tsukuba, Ibaraki 305-0003, Japan

Received: June 12, 2003

Abstract. We propose a method to synthesize oxide nanoparticles in insulators by oxidizing metal nanoparticles which introduces less damage comparing with commonly used sequential implantation of metal ions and oxygen ions. Nanoparticles of Ni and Cu were fabricated in SiO_2 by the negative ion implantation, and were oxidized in O_2 gas flow at 600 – 1000 °C for 1 hr. The oxidized nanoparticles were evaluated using optical absorption spectroscopy, SQUID magnetometry and Rutherford backscattering spectrometry (RBS), in comparison with annealed samples in vacuum at the same temperatures. Whereas the vacuum-annealed Ni nanoparticles show a broad absorption over visible and ultraviolet regions, the O_2-annealed Ni nanoparticles, i.e., oxidized ones, become transparent in the visible region and show a steep absorption edge around ~4 eV. A strong ferromagnetic signal of Ni nanoparticles disappears after the oxidation. These results strongly indicate formation of NiO. In the case of Cu nanoparticles, the absorption spectra do not significantly change, except disappearance of a surface plasmon resonance (SPR) peak after oxidation. The oxidation drastically improves thermal stability against high-temperature diffusion.

1. INTRODUCTION

Metal nanoparticles dispersed in insulators draw much attention, because of applicability for optical switches [1] and single electron transistors [2], etc. Negative-ion implantation is one of the promising methods to fabricate nanoparticles in insulators, without heat treatment, with good controllability inherent in ion implantation and without surface charging [3,4]. Up to now, we have succeeded in fabricating Cu nanoparticles in amorphous SiO_2 and some other insulators [5-7], in observing large optical nonlinearity [8], ultra-fast response [9] and single electron transport [10]. One of the next goals is addressed to formation of *compound* nanoparticles in insulators using the high-flux negative-ion implantation method. Already some groups have partially succeeded in fabrication of compound nanoparticles of GaAs [11], Cu_2O [12], CuCl [13], VO_2 [14], etc., using sequential (positive) ion implantation. However, in some cases, secondary implantation of the sequence induces too much enhanced diffusion of the primary implanted atoms, and prevents the compound formation. Even, succeeding in the formation, the compound nanoparticles may contain a lot of defects. In this paper, an alternative method, which is only applicable to oxide compounds, but introduces less defects, i.e., oxidation of metal nanoparticles, is examined.

2. EXPERIMENTAL

Optical-grade KU-1 silica glasses (OH^-: 820 ppm) of 15 mm in diameter and 0.5 mm in thickness were implanted with Ni or Cu negative ions of 60 keV from a Cs-assisted plasma-sputter type high-flux ion source [4]. The ion fluxes and the doses ranged in 1–60 $\mu A/cm^2$ and $3 \cdot 10^{16}$ –$1 \cdot 10^{17}$ ions/cm^2, respectively. According to SRIM2000 code [15], the projected range and the straggling of Ni (Cu) ions of 60

Corresponding author: H. Amekura, e-mail: amekura.hiroshi@nims.go.jp

keV are 47 (46) nm and 16 (15) nm in SiO_2, respectively.

Heat treatments were carried out at 400–1000 °C for 1 hr in a tube furnace, in *vacuum* of a base pressure less than $1 \cdot 10^{-3}$ Pa or in *oxygen gas flow* of ~ 100 sccm under nearly atmospheric pressure.

A dual-beam spectrometer with a resolution of 1 nm was used for measurements of the transmittance and the reflectance in the wavelength range of 190–1700 nm at room temperature. Absorption (optical density) spectra free from the incoherent multiple reflection (ICMR) in samples were obtained from three sets of measurements [8,16]: The transmittance $\Theta_T = I_T / I_0$, reflectance of the implanted surface side $\Theta_R = I_R / I_0$ and reflectance of the rear surface side $\Theta_R' = I_R' / I_0$, were measured on the same samples, where I_0, I_T, I_R and I_R' denote intensities of incident light, transmitted light, reflected light of the implanted surface and reflected light of the rear surface, respectively. The ICMR-free transmittance of the implanted layer T and the ICMR-free reflectance of the implanted surface side R_1 are expressed as,

$$T = \frac{\Theta_T (R_0 - 1)}{\left\{ R_0 (2 - \Theta_R') - 1 \right\} \exp(-\alpha_S d_S)}, \qquad (1)$$

$$R_1 = \Theta_R + \frac{R_0 \Theta_T^2}{R_0 (2 - \Theta_R') - 1}, \qquad (2)$$

where d_S, R_0 and α_S denote substrate thickness, reflectance and absorption coefficient of unimplanted substrate, respectively [8,16]. We define optical density (OD) ad of the implanted layer as,

$$\alpha d = -\ln\left(\frac{T}{1 - R_1} \right). \qquad (3)$$

where α and d denote absorption coefficient and effective thickness of the implanted layer [16]. A reference path of the dual-beam spectrometer was kept vacant.

Several pieces of (2-3)×(2-3.5)×0.5 mm^3 were cut from the implanted samples, and were inserted into a Superconducting Quantum Interference Device (SQUID) magnetometer. Magnetic field (H) dependence was measured in H = 0–50 kOe at T = 300K.

Rutherford Backscattering Spectrometry (RBS) was conducted to evaluate depth profile changes of the Ni and Cu atoms after heat-treatments, using 2.06 MeV He^+ beam of 1 mm ϕ in diameter with a scattering angle of 160 degrees. To reduce charging of substrates, samples were covered by Al foils except evaluation spots.

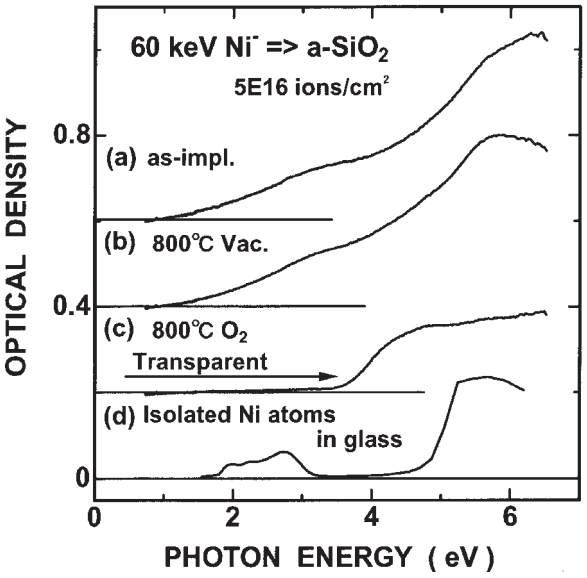

Fig. 1. Optical absorption spectra of SiO_2 implanted with Ni^- ions of 60 keV, in (a) as-implanted state, and after annealing at 800 °C for 1 hr in (b) vacuum and (c) O_2 gas flow. A spectrum of isolated Ni atoms in silicated glass from Ref. [20] is also shown in (d).

3. RESULTS

3.1. Nickel case

Silica glasses (SiO_2) implanted with Ni^- ions of 60 keV to $5.5 \cdot 10^{16}$ ions/cm^2 show dark brownish color in as-implanted state. Even after annealing in *vacuum* at 800 °C for 1 hr, the color does not change. However, annealing in O_2 *gas* at 800 °C for 1 hr bleaches the color completely. The change is clearly seen in optical absorption spectra in Fig. 1. Two broad peaks at 3.3 eV and 5.8 eV are characteristic in formation of metallic Ni nanoparticles in SiO_2 [16,17]. The vacuum annealing at 800 °C induces almost no changes except absorption around 6 eV which is probably due to defect annihilation [16]. However, the oxygen annealing at 800 °C extends a transparent region over the visible region up to 3.5 eV. According to isochronal annealing in O_2 gas flow for 1 hr each, the spectrum does not change up to 400 °C. After 600 °C annealing, the spectrum is similar with that of 800 °C, i.e., a plateau absorption from 4.5 to 6.5 eV instead of the 5.8 eV peak due to Ni nanoparticles. However, a weak absorption is still

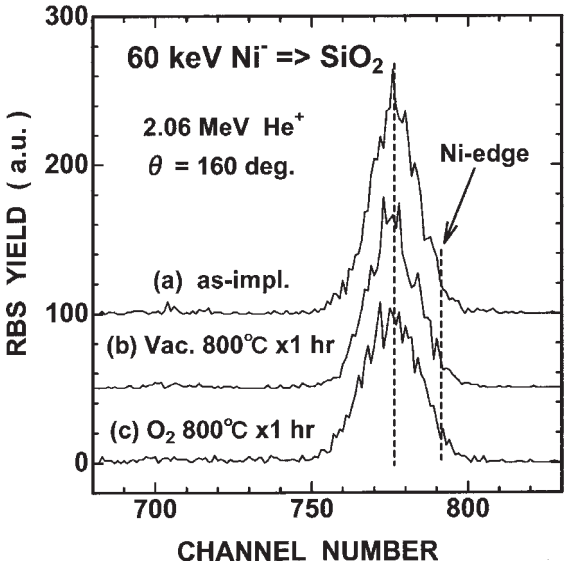

Fig. 2. RBS spectra of SiO_2 implanted with Ni^- ions of 60 keV, in (a) as-implanted state, and after annealing at 800 °C for 1 hr in (b) vacuum and (c) O_2 gas flow.

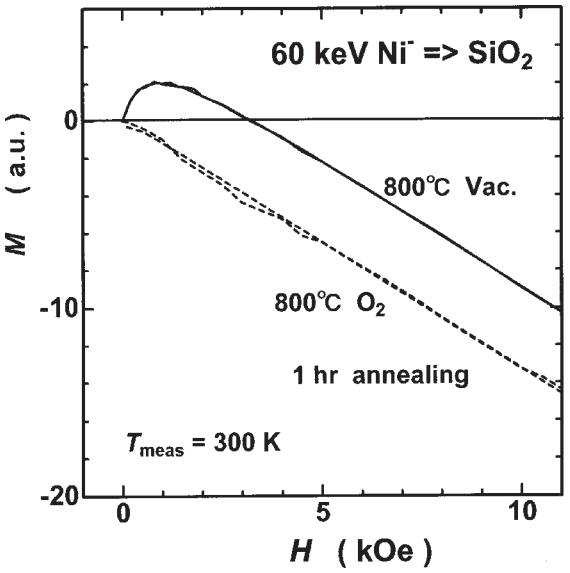

Fig. 3. Field dependence of magnetization M of SiO_2 implanted with Ni^- ions of 60 keV, after annealing at 800 °C for 1 hr in vacuum (solid lines) and O_2 gas flow (dotted lines). Both the curves with increasing and decreasing field are shown.

observed in the visible region even after 600 °C annealing. At 700 °C, transparency up to ~3.5 eV is attained.

Fig. 2 shows RBS spectra of Ni edge in as-implanted, vacuum- and O_2-annealed samples, which correspond to depth distribution of Ni atoms beneath the surface. The Ni edge shown as an arrow corresponds to the surface position. Comparing with the as-implanted state, Ni peak concentration slightly decreases in both the vacuum- and the O_2-annealed samples. The profile of the O_2-annealed sample slightly becomes wider. However, most of Ni atoms still remain in a similar depth with the as-implanted state. The drastic changes in absorption spectra are not due to decreases of Ni atoms in the sample.

Fig. 3 shows field dependence of magnetization of SiO_2 implanted with Ni^- ions of 60 keV, measured at room temperature after vacuum and O_2 annealing at 800 °C for 1 hr. The field dependences were recorded with both increasing and decreasing the field. No hysteresis was observed within experimental errors. Both the samples show negative magnetization at high fields, because of diamagnetic signal of SiO_2 matrices. The vacuum annealed samples shows positive magnetization at weak fields, which is due to ferromagnetic signal from Ni metallic nanoparticles. Although the magnetization turns to decrease exceeding 1 kOe, it is reasonable because the ferromagnetic signal saturates less than 1 kOe.

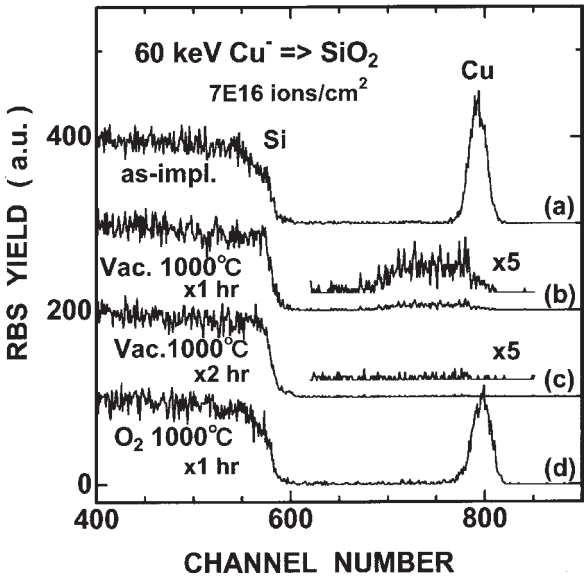

Fig. 4. RBS spectra of SiO_2 implanted with Cu^- ions of 60 keV, in (a) as-implanted state, and after annealing at 1000 °C in (b) vacuum for 1 hr, (c) vacuum for 2 hr, or (d) O_2 gas flow for 1 hr.

The as-implanted sample (not shown in Fig.) shows a similar behavior [17]. Field dependence of the O_2-annealed sample is almost similar to that of an unimplanted SiO_2. Results observed in the O_2 annealed sample are not inconsistent with a weak linear positive signal expected from antiferromagnetic NiO.

Disappearance of the hysteresis is due to superparamagnetic behavior of Ni metallic nanoparticles in the vacuum annealed sample, and due to antiferromagnetic nature of NiO nanoparticles in the O_2 annealed sample. The O_2 annealing drastically changes the magnetic properties of Ni implanted SiO_2.

3.2. Copper case

Copper nanoparticles are oxidized by O_2 annealing for 1 hr at 600 °C or higher. Since the band-gap energy of Cu_2O is ~2 eV, similar to the absorption edge of Cu metal nanoparticles, a drastic shift of absorption spectrum cannot be observed. Just the SPR peak disappeared after oxidation.

Once metal nanoparticles are converted to the oxides, thermal stability against high temperature diffusion is improved. This tendency is somewhat observed in Ni case, but is more pronounced in the Cu case. The results are summarized in Fig. 4. The Cu nanoparticles in SiO_2 are unstable against vacuum annealing at 1000 °C or higher [18,19], as shown in Fig. 4 as disappearance of Cu RBS signal. Enhanced diffusion of Cu atoms results in disappearance of Cu atoms in SiO_2. However, Cu atoms stably exist in SiO_2 even at 1000 °C with O_2 atmosphere.

4. DISCUSSION

One might consider the observed absorption changes in the Ni implanted SiO_2 was due to isolated Ni ions which would be dispersed in SiO_2 after destruction of Ni nanoparticles under O_2 annealing. Fig. 1(d) shows a spectrum from the isolated Ni atoms in silicate glass [20]. Structures at 2 ~ 3 eV are characteristic in the isolated Ni atoms. Since the structures are not observed in the O_2 annealed samples, the destruction of Ni nanoparticles to isolated atoms is not the case. It should be noted that the structures at 2 ~ 3 eV was not observed also in the as-implanted state. According to an estimation, ~85% of implanted Ni atoms form nanoparticles even in the as-implanted state [21].

As shown in a previous paper [17], Ni silicide particles, at least NiSi, Ni_2Si and Ni_3Si, in SiO_2 are not transparent in visible region. Since band-gap energy of Ni oxide (NiO) is ~4 eV, the spectrum change is well explained as formation of NiO. The formation of NiO is consistent with the magnetic behaviors. Thus, we have succeeded in the synthesis of metal oxide in SiO_2, using thermal oxidation of metal nanoparticles.

5. CONCLUSION

Using Ni and Cu nanoparticles in SiO_2 as examples, we have shown that thermal oxidation drastically modifies optical, magnetic and thermodynamic properties of metal nanoparticles via oxide nanoparticle formation. Metal nanoparticles of Ni and Cu in SiO_2 fabricated by the negative ion implantation were oxidized in O_2 gas flow at 600 – 1000 °C for 1 hr. Although the vacuum-annealed Ni nanoparticles show a broad absorption over visible and ultraviolet regions, the oxidized Ni nanoparticles become transparent in visible region and show a steep absorption edge around ~4 eV. The oxidation changes the magnetic properties, i.e., a strong ferromagnetic magnetization of Ni nanopariticles disappears after the oxidation. Observed changes in optical and magnetic properties strongly indicate the formation of NiO. In the case of Cu nanoparticles, the absorption spectra do not significantly change, except disappearance of a surface plasmon resonance (SPR) peak after oxidation. The oxidation improves thermal stability against high-temperature diffusion around 1000 °C.

ACKNOWLEDGEMENT

A part of this study was financially supported by the Budget for Nuclear Research of the MEXT, based on the screening and counseling by the Atomic Energy Commission.

REFERENCES

[1] R.F. Haglund, L. Yang, R.H. Magruder, C.W. White, R.A. Zhur, L. Yang, R. Dorsinville and R.R. Alfano // *Nucl. Instr. and Meth.* **B91** (1994) 493.

[2] A. Nakajima, H. Nakao, H. Ueno, T. Futatsugi and N. Yokoyama // *Appl. Phys. Lett.* **73** (1998) 1071.

[3] J. Ishikawa, H. Tsuji, Y. Toyota, Y. Gotoh, K. Matsuda, M. Tanjyo and S. Sakaki // *Nucl. Instr. and Meth.* **B96** (1995) 7.

[4] N. Kishimoto, Y. Takeda, V.T. Gritsyna, E. Iwamoto and T. Saito, In: *IEEE Trans. from 1998 Int. Conf. on Ion Impl. Tech. Proc.*, ed. by J. Matsuo, G. Takaoka and I. Yamada (IEEE: Piscataway, 1999), p. 342.

[5] N. Kishimoto, V.T. Gritsyna, K. Kono, H. Amekura and T. Saito // *Mat. Res. Soc. Symp. Proc.* **438** (1997) 435.

[6] N. Kishimoto, Y. Takeda, N. Umeda, V.T. Gritsyna, C.G. Lee and T. Saito // *Nucl. Instr. and Meth.* **B166-167** (2000) 840.

[7] Y. Takeda, C.G. Lee and N. Kishimoto // *Nucl. Instr. and Meth.* **B191** (2002) 422.
[8] Y. Takeda, V.T. Gritsyna, N. Umeda, C.G. Lee and N. Kishimoto // *Nucl. Instr. and Meth.* **B148** (1999) 1029.
[9] Y. Takeda, J.P. Zhao, C.G. Lee, V.T. Gritsyna and N. Kishimoto // *Nucl. Instr. and Meth.* **B166-167** (2000) 840.
[10] H. Amekura, N. Umeda, Y. Takeda, N. Kishimoto and H. Nejyo, In: *Proc. of 5th Int. Symp. on Adv. Phys. Fields*, ed. by K. Yoshihara (NRIM: Tsukuba, 2000) p. 203.
[11] S. Okamoto, Y. Kanemitsu, K.S. Min and A. Atwater // *Appl. Phys. Lett.* **73** (1998) 1829.
[12] S. Nakao, K. Saitoh, M. Ikeyama, H. Niwa, S. Tanemura, Y. Miyagawa, S. Miyagawa, M. Tazawa and P. Jin // *Nucl. Instr. and Meth.* **B141** (1998) 246.
[13] K. Fukumi, A. Chayahara, N. Kitamura, T. Akai, J. Hayakawa, K. Fujii and M. Satou // *J. Non-Cryst. Solids* **178** (1994) 155.
[14] R. Lopez, T.E. Haynes, L.A. Boatner, L.C. Feldman and R.F. Haglund // *Opt. Lett.* **27** (2002) 1327.
[15] J.F. Ziegler, J.P. Biersack and U. Littmark, *The Stopping and Range of Ions in Solids* (Pergamon Press, New York, 1985), Chap. 8.
[16] H. Amekura, Y. Takeda, H. Kitazawa and N. Kishimoto // *Proc. SPIE* **4977** (2003) 639.
[17] H. Amekura, H. Kitazawa, T. Mochiku, N. Umeda, Y. Takeda and N. Kishimoto // *Proc. SPIE* **4936** (2002) 1.
[18] N. Umeda, N. Kishimoto, Y. Takeda, C.G. Lee and V.T. Gritsyna // *Nucl. Instr. and Meth.* **B166-167** (2000) 864.
[19] H. Amekura and N. Kishimoto // *J. Appl. Phys.* **94** (2003) 2585.
[20] C. Estourenes, T. Lutz and J.L. Guille // *J. Non-Cryst. Solids* **197** (1996) 192.
[21] H. Amekura, H. Kitazawa and N. Kishimoto // submitted to *Nucl. Instr. and Meth. B.*